

Polytechnic Institute of New York

AERODYNAMICS
LABORATORIES
~
DEPARTMENT OF MECHANICAL
and
AEROSPACE ENGINEERING

THE APPLICABILITY OF BRILLOUIN SCATTERING TO FLOW FIELD DIAGNOSTICS

NASA-CR-158017
19790010112

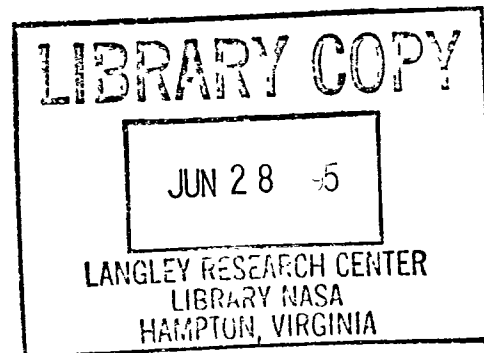
By J. Laiosa and S. Lederman

FINAL REPORT

FEBRUARY 1979

Grant NSG 1198

Approved for public release;
distribution unlimited.



POLY M/AE Report No. 79-10



THE APPLICABILITY OF BRILLOUIN SCATTERING
TO FLOW FIELD DIAGNOSTICS



FINAL REPORT

by J. Laiosa and S. Lederman

Prepared For
NATIONAL AERONAUTICS AND SPACE ADMINISTRATION
Langley Research Center
Hampton, Virginia

Grant No. NSG-1198

S. Lederman, Principal Investigator

July 1, 1976 - June 30, 1977 78⁷

POLYTECHNIC INSTITUTE OF NEW YORK
Aerodynamics Laboratories
February 1979

POLY M/AE Report No. 79-10

N79-18283#

TABLE OF CONTENTS

<u>Section</u>	<u>Page</u>
Nomenclature	ii
List of Figures	v
I - Introduction	1
II - Theory	3
A. Hydrodynamic limit	6
B. Kinetic limit	8
III - Experimental Criteria	9
IV - Experimental Equipment	12
V - Gas Sample Preparation and Technique	15
VI - Findings	16
VII - Conclusion	21
VIII - References	23
IX - Bibliography	25
Figures	26-

THE APPLICABILITY OF BRILLOUIN SCATTERING TO FLOW FIELD DIAGNOSTICS

FINAL REPORT

by

J. Laiosa and S. Lederman

ABSTRACT

To fill the void between turbulence theory and experiment; particularly in the flow fields consisting of monoatomic gases, for example in wind tunnels, means of measuring fluctuating quantities are needed. In the area of density fluctuation measurement, the optical method of Brillouin scattering has been suggested. This was based on the theory, that the Brillouin scattered intensity is proportional to a function of density. This function can be shown to be the density-density correlation function, $\langle \hat{\rho}(k, \omega) \rho(-k) \rangle$. In this investigation the potential of this method as a diagnostic tool was studied. Here the density fluctuations in gases were sought. Continuous wave lasers and interferometers were used as the primary illuminating source and scattered light filters respectively.

NOMENCLATURE

c	speed of light, 2.9973×10^{10} cm/sec
c_p	specific heat at constant pressure
c_v	specific heat at constant volume
c_{rot}, c_{vib}	rotational and vibrational specific heats
c_{tr}	translational specific heat, for monoatomic gas, $c_{tr} = c_v$
D	self-diffusion constant
ϵ	dielectric constant

$\hat{\epsilon}$	Fourier-Laplace transform of the dielectric constant
f, f_0	kinetic distribution function, equilibrium value
h	perturbed quantity of the kinetic distribution function
i	imaginary number, $i = \sqrt{-1}$
I, I_0, I_C, I_B	scattered intensity, incident radiation, central line intensity, Brillouin line intensity
k, k_i, k_s	change in wave propagation vector, incident and scattered wave propagation vector
k_b	Boltzman's constant, 1.38×10^{-16} ergs/°K
m	molecular mass
N	number of molecules
P	pressure
\bar{p}	momentum
q	kinetic energy
\bar{r}	position vector
R	molecular gas constant
$S(\bar{k}, \omega)$	generalized structure factor
T, T_0, T_1	temperature, equilibrium value, fluctuating value, $T = T_0 + T_1$
t	time
τ_{rot}	rotational relaxation time
τ_{vib}	vibration relaxation time
τ'	modified rotational relaxation time, $\tau' = \frac{C_{tr}}{C_{tr} + C_{rot}} \tau_{rot}$
τ''	modified vibration relaxation time, $\tau'' = \frac{C_{tr} + C_{rot}}{C_{tr} + C_{rot} + C_{vib}} \tau_{vib}$
\bar{u}	velocity vector
u_1	longitudinal component of the velocity

v_o	speed of sound
y	non-dimensional parameter
$y(\bar{u}, F, t)$	general thermodynamic parameter
α	polarizability
α_T	thermal diffusivity
β	thermal expansion coefficient
η_s	shear viscosity
η_B	bulk viscosity
$\eta_{B\text{CLASS}}$	classical bulk viscosity
η_B^{vib}	vibrational bulk viscosity
η_B^{rot}	rotational bulk viscosity
ρ	density
λ	wavelength of light
λ_T	thermal conductivity
λ_C	mean free path
λ_S	wavelength of scattered light
Ω	angular frequency of scattered light
ϕ	angle between point of observation and electric field vector
ω	shift in angular frequency
ν	frequency
γ	ratio of specific heats
θ	angle between incident wave vector and point of observation

LIST OF FIGURES

<u>Figure</u>		<u>Page</u>
1	The Stratified Medium Model and the "Coherent Reflection" of Light	
2	Limits of the Hydrodynamic and Kinetic Regions for Helium and Xenon at Various Scattering Angles	
3	Theoretical Hydrodynamic Brillouin Spectrum	
4	Brillouin Spectrum as a Function of γ	
5	Schematic View of the Experimental Equipment	
6	Pictorial View of the Experimental Equipment	
7	Mode 590 Jet Stream Dye Laser Optical Schematic	
8	Presetting the Fabry-Perot Interferometer	
9	Spectral Response of Dye Laser. Free Spectral Range is 3GHz. Laser Bandwidth of Half Intensity is 250MHz	
10	Spectral Response of Argon-ion Laser Line. Laser Bandwidth at Half Intensity is 125MHz	
11	Apparent Spectrum Obtained from Water	
12	Spectral Response from Absolute Alcohol	

I - INTRODUCTION

In the past probes, such as hot wires, thermocouples, pitot tubes and sampling probes, were used to obtain good results for average values of fluid parameters. While it is true, some of these methods could be used to obtain the fluctuating values of fluid parameters, care must be taken to eliminate the fluctuations due to the probe itself. This is not easily done since its effects are not always known apriori. Therefore one has sought other means of investigating fluid flows. This train of thought spurred the development of non-intrusive optical techniques¹. These methods can be sub-divided into two classes, indirect (or "path") methods and direct (or "point") methods. In the area a density fluctuation measurement, methods of the first type include absorption-emission, Interferometry and Holography. The second type include such methods, as Raman scattering, Rayleigh scattering and florescence.

In the "path" methods one has to contend with diagnosing only 2-dimensional or axis-symmetric flows. This is due to interaction of light and fluid occurring along the entire beam length. Therefore the whole beam is the scattering volume. The techniques for extracting information from the scattered light are mathematically difficult. Not only are they difficult to implement, these techniques closely resemble the turbulent modeling. Therefore, why not numerically model the flows instead of experimentally trying to measure them.

In the area of direct or "point" techniques, Raman scattering has emerged as a useful and accurate method for determining point-wise concentrations in flow fields. But for fluctuation measure-

ments a costly high power laser is needed. In addition, Raman scattering is applicable only to polyatomic molecules which are Raman active. Monoatomic molecules do not exhibit Raman activity.

In light of this it would be desirable to have a method that would produce a higher level of scattering and at the same time be sensitive also to monoatomic molecules. With this, a relatively low cost continuous wave (cw) laser could be used to monitor the fluid as a function of time.

At the outset of this investigation, it was believed Brillouin scattering could accomplish this feat. In the past, Brillouin scattering has been used to measure sound speeds in gases^{2,3}.

The procedure used to monitor the density fluctuations involves the use of a high resolution interferometer in an unconventional mode of operation. Usually a sawtooth is applied to the piezoelectric drive which provides the sweep over a narrow bandwidth corresponding to the free spectral range of the interferometer. If a single voltage is applied, theoretically a single frequency should pass through the mirrors. Therefore, by prebiasing the interferometer at a particular voltage a particular frequency of light will be transmitted. And since the intensity of this light is proportional to the density of the fluid, a measure of the variation of this scattered light would indicate the fluctuation in the density of the fluid. In an earlier investigation⁴ an attempt was made to measure density fluctuations in liquids, but due to quality of the equipment available, and the difficulty of purifying these liquids, no conclusion could be drawn at that time. Therefore, new equipment was obtained and the interest was shifted to gases since it was believed the gases could be easily purified. The interest in gases was also sparked

by the fact that it is the primary type of fluid used in fluid dynamic flow fields. Liquids were only introduced because their scattering is more intense and therefore an easy point to begin an investigation.

While a Rayleigh-Brillouin spectrum could not be detected, some ✓ reasons were discovered that implied the inadequacy of Brillouin scattering as a diagnostic tool at the present time.

In the following section a brief account of the theoretical aspects of Brillouin scattering is shown. The following section provides the experimental criteria needed for a successful experiment. After a description of the equipment involved, the reasons for discounting Brillouin scattering to measure density fluctuations are given.

II - THEORY

The phenomena of Brillouin scattering is the result of light scattering from density fluctuations present in the fluid. Brillouin⁴ first implied that light is elastically scattered from thermal sound waves produced by the medium. These sound waves create stratified layers consisting of alternating planes of compression and rarefaction wave forms (see Fig. 1).

Due to momentum conservation requirements, the change in wave propagation vector is given by

$$\bar{K} = \bar{K}_i - \bar{K}_s \quad (1)$$

The magnitude of \bar{K} can be expressed as

$$|\bar{K}| = 2|\bar{K}_i| \sin \theta/2 \quad (2)$$

since $|\bar{K}_i| \approx |\bar{K}_s|$.

Also, in the presence of the translational motion of the molecules, the scattered light is Doppler shifted. This shift is given by

$$\Delta\nu = \frac{kV_o}{2\pi} = \frac{2V_o \sin\theta/2}{\lambda_o} \quad (3)$$

The scattered light intensity can be expressed in many ways. Kamarov and Fisher⁶ have adapted Van Hove's⁷ neutron-scattering to light scattering. Their expression for the scattered light intensity is:

$$I(\bar{r}, \omega) = (\alpha^2 \Omega^4 N / 2\pi c^4 r^2) I_{os} \sin^2 \phi S(\bar{K}, \omega) \quad (4)$$

The generalized structure factor S can be expressed:

$$S(\bar{k}, \omega) = 2R_e \langle \hat{\epsilon}(\bar{k}, i\omega) \hat{\epsilon}(-\bar{k}) \rangle \quad (5)$$

Where $\hat{\epsilon}$ is the Fourier-space Laplace-time transform of the dielectric constant ϵ . Therefore one needs to express the behavior of ϵ , for the medium. Fortunately the change in ϵ can be expressed as the change in any two thermodynamics parameters. If density and temperature are selected, one obtains:

$$\delta\epsilon(\bar{r}, t) = \left(\frac{\partial\epsilon}{\partial\rho}\right)_T \delta\rho(\bar{r}, t) + \left(\frac{\partial\epsilon}{\partial T}\right)_\rho \delta T(\bar{r}, t) \quad (6)$$

This can be further simplified since the temperature dependence is small as compared to the density dependence⁹. Therefore the problem rests on obtaining an expression for $\delta\rho(\bar{r}, t)$.

Due to the diverse nature of dense fluids and gaseous fluids, two regions exist where different solutions apply. Hence, $\delta\rho$ may be obtained in different manners for each region. Before discussing these methods, it would be advantageous for one to know in which region a particular fluid resides. This is important since a gas can be in either region depending on its thermodynamical properties and the scattering angle used for viewing.

To distinguish between the two regions, one should consider the collisional rate process which differs vastly for each. With this, one can intuitively see the validity of the parameter "y" as an indicator of the region in which the fluid resides for a particular case⁸. This parameter is expressed as:

$$y = \lambda_s / \lambda_c = (2\pi/k) / \lambda_c \quad (7)$$

Here y is seen to be the ratio of wavelength of the fluctuations observed to the collisional mean free path.

Therefore for $y \gg 1$, the wavelength of the fluctuations is much larger than the mean free path. This regime is denoted the "Hydrodynamic regime" since it is governed by the hydrodynamic equations of motion.

For $y \ll 1$, the fluctuation wavelength is much shorter than the mean free path. Since the collisions are very infrequent, the system can no longer be considered a continuum. Hence, this is denoted as the "kinetic regime". This variation of y can be viewed graphically by considering Fig. 2, (Ref. 4). Here the parameter y is shown for two monoatomic molecules, Helium and Xenon at two scattering angles, 10° and 160° . As stated earlier, each molecule can be in either regime depending on k (scattering angle) and its density. This can also be seen in the above figure.

Now that the distinction between the two regimes has been defined, an expression for $\delta\rho$ for each regime is possible. Before these expressions for $\delta\rho$ are given, the spectral shape of the scattered light for each domain will be discussed. In the hydrodynamic region the spectrum consists of three components, (see Fig. 3). The central component is the unshifted Rayleigh line. Straddling this central line are the two Brillouin lines. The existence of two lines is due to the oscillations of the thermal sound waves in both longitudinal directions. The ratio of intensities of this spectrum can be expressed as

$$\frac{I_C}{2I_B} = \gamma - 1 \quad (8)$$

where I_C and I_B are the intensities of the central and Brillouin lines respectively. This equation actually holds where relaxation

effects are negligible, but it gives a good result for relative differences in the intensities of the central and Brillouin peaks. As one proceeds into the kinetic region (y decreasing), the lines come closer together. This can be seen in Fig. 4 taken from Ref. 4. Here it is seen at a value of $y = 2.0$ the lines are still separated, but at $y = 1.0$ the lines are almost indistinguishable. Finally at $y = 0.5$, no distinct line is visible. Also, the maximum intensity tends to decrease as y decreases.

In the sections that follow, a brief statement of the derivation of $\delta\rho$ for both regimes is given. These derivations are taken primarily from Ref. 10 & 11. The interested reader can consult these references for a more descriptive explanation.

A. Hydrodynamic Limit

For a dense fluid, the linearized hydrodynamic equations of motion¹² are the continuity equation:

$$\frac{\partial \rho_1}{\partial t} + \rho_0 \operatorname{div} \bar{u} = 0 \quad (9)$$

the longitudinal component of the Navier-Stokes equation:

$$\rho_0 \frac{\partial u_1}{\partial t} + \frac{v_0^2}{\gamma} \operatorname{grad} \rho_1 + \frac{v_0^2 \beta \rho_0}{\gamma} \nabla T_1 - \left(\frac{4}{3} \eta_s + \eta_B \right) \operatorname{grad} \operatorname{div} \bar{u} = 0 \quad (10)$$

and the energy transport equation:

$$\rho_0 c_v \frac{\partial T_1}{\partial t} - \frac{c_v (\gamma - 1)}{\rho} - \frac{\partial \rho_1}{\partial t} \lambda_T \nabla^2 T_1 = 0 \quad (11)$$

From here one can obtain the Fourier-space Laplace-time transform of the density fluctuations. This can be accomplished by first taking the divergence of Eq. 5 and substituting for $\nabla \cdot \bar{u}_1$ from Eq. 4. Then the Fourier-Laplace transforms can be obtained for $\delta\rho$

(see Refs. 11,13). The final result for the intensity can be obtained numerically or by several approximate analytical methods.

The above theory provided satisfactory results for monoatomic fluids. For polyatomic fluids, the theory differed appreciably from experiment. Neglect of the other forms of internal degrees of freedom (rotational and vibrational) was the reason for this discrepancy.

The inclusion of these effects can be made by introducing a frequency dependent bulk viscosity and a self diffusion dependent thermal conductivity in the given hydrodynamic equations. For the bulk viscosity we have

$$\eta_B = \eta_{B_{CLASS}} + \eta_B^{vib} + \eta_B^{rot} \quad (12)$$

where $\eta_{B_{CLASS}}$ is the usual bulk viscosity and

$$\eta_B^{rot} = \frac{PRC_{rot} \tau_{rot}}{(C_{rot} + C_{tr})^2} \frac{1}{1+i\omega\tau} \quad (13)$$

$$\eta_B^{vib} = \frac{PRC_{vib} \tau_{vib}}{C_r^o^2} \frac{1}{1+i\omega\tau} \quad (14)$$

are the rotational and vibrational bulk viscosities respectively¹². As for the thermal conductivity, one has the following expression

$$\lambda_T = \eta_s \left[\frac{5}{2} C_{tr} + \rho_o D (C_{rot} + C_{vib}) \right] \quad (15)$$

With these modifications, the scattering from a polyatomic fluid can be accurately predicted.

As a final note, theories have been developed for binary gas mixtures. These theories can be seen in Refs. 11 and 16.

B. Kinetic Limit

In the kinetic regime, one must express the density distribution in a manner compatible to with the theory of rarefied gases. For a monoatomic gas, the molecular distribution is given by

$$dN(\bar{u}, \bar{r}, t) = f(\bar{u}, \bar{r}, t) d\bar{r} d\bar{u} \quad (16)$$

Here dN is the number of molecules with the coordinates (\bar{u}, \bar{r}, t) within the spatial volume $d\bar{r}$ and velocity volume $d\bar{u}$. With this distribution, any macroscopic parameter can be determined. This can be seen if one considers $y(\bar{r}, \bar{u})$ as any one of those parameters. Then

$$\langle y(\bar{r}, t) \rangle = \int f(\bar{u}, \bar{r}, t) y(\bar{r}, \bar{u}) d\bar{u} \quad (17)$$

If y is a power^{function} of the velocity only, it is then considered a moment of the function f . In the collisional process there are several moments of physical interest. These are:

$$\langle y_1 \rangle = \rho = m \int f d\bar{u} \quad (\text{mass density}) \quad (18a)$$

$$\langle y_2 \rangle = \bar{p} = m \int f \bar{u} d\bar{u} \quad (\text{momentum density}) \quad (18b)$$

$$\langle y_3 \rangle = q = \frac{m}{2} \int f \bar{u}^2 d\bar{u} \quad (\text{kinetic energy density}) \quad (18c)$$

One can linearize the function f in the following form:

$$f(\bar{u}, \bar{r}, t) = f_0(\bar{u}) [1 + h(\bar{u}, \bar{r}, t)] \quad (19)$$

The functional relation f_0 is the equilibrium distribution given by the Maxwell distribution as

$$f_0(\bar{u}) = n_0 (m/2\pi k_B T_0)^{3/2} \text{EXP}(-m\bar{u}^2/2k_B T_0) \quad (20)$$

Therefore, the function $h(\bar{u}, \bar{r}, t)$ is the perturbed quantity. If this expression for f is substituted into the governing Boltzman equation,

one obtains

$$\left(\frac{\partial}{\partial t} + \bar{\mathbf{u}} \cdot \nabla\right) h = \left(\frac{\partial h}{\partial t}\right)_{\text{COLL}} \quad (21)$$

Hence, the local density fluctuation is given by

$$\delta\rho(\bar{\mathbf{v}}, t) = m \int f_0(\bar{\mathbf{u}}) h(\bar{\mathbf{u}}, \bar{\mathbf{r}}, t) d\bar{\mathbf{u}} \quad (22)$$

Therefore, to determine the density fluctuation one needs to determine the expression for the perturbation function h . This procedure is a long, tedious mathematical journey. Since it is not the purpose of this work to rederive the existing theory, it will not be given here. References 8,9 and the papers listed in the Bibliography, can be examined for a more thorough explanation.

III - EXPERIMENTAL CRITERIA

In the discussion that follows, the specifications required of the experimental equipment are given. These requirements are actually those needed to measure a Rayleigh-Brillouin spectrum, but oddly enough, most of these requirements (mainly the stability) are also needed to monitor density fluctuations which is the purpose of this investigation. In addition to these basic specifications, one major requirement of the frequency filtering device is also needed. This requirement will be discussed after the basic specifications are given.

As in all light scattering techniques, the need for a reliable and stable monochromatic light source is obvious. Due to the nature of the Rayleigh-Brillouin phenomenon, the above requirements should be redefined and new specifications examined. These requirements can be obtained by considering the difference of Brillouin scattering over the various other techniques.

In Rayleigh-Brillouin scattering, the entire spectrum is confined to a very small frequency range. One can visualize this if a simple calculation is performed for the spectrum of a typical substance. If nitrogen is taken as an example, at $T = 300^\circ\text{K}$ the shift

becomes 97.07MHz and the halfwidth 34.2MHz.

The next important factor is the low light level of the scattered radiation. This may seem to be a contradiction to what has been said earlier, but it is not. The reason being, in most light scattering density measurement methods a high power pulsed laser is used. (For example in Raman scattering techniques). Here a relatively low power continuous wave laser is used. The CW laser was selected since one is interested in a continuous spectrum. Also its large scattering cross-section should compensate for the reduction in power. Through the course of this experiment (and through some literature research),^{8,9} it is discovered that either long running times, 15-30 minutes, or repetitive scans were necessary to detect a spectrum. Therefore the larger Brillouin scattering cross-section did not completely compensate the reduction in power.

Keeping the above aspects of the Rayleigh-Brillouin scattering process in mind, some basic equipment requirements can be established.

In regard to reliability, one cannot expect trouble free use of a highly complex instrument such as a laser. But after a period of debugging, it should operate with a minimum of problems providing the proper maintenance is performed.

As for stability, there is actually two main types. These are energy output and frequency stability. In CW light scattering techniques, it is usually difficult to take into account variations in incident light energy. This involves some sort of two channel correlation. Therefore it is usually required that the energy doesn't fluctuate more than a few percent over the period of the experiment. In some applications where a fluctuating parameter is being monitored, the laser fluctuation can outweigh the physical

variation.

Before the frequency stability requirement is discussed the area of laser line width should be explored. As can be seen by the calculations presented earlier, the laser line width should be less than 68.4MHz (twice the halfwidth). Typically this is not found in most lasers without the use of an etalon. Care must be taken when incorporating an etalon. This adds an additional area where the stability of the system can be affected. Returning to the question of laser line width, one could ask how narrow should the width be? This is difficult to estimate. A safe value of 30-40MHz is advised.

Since long running times or repetitive scans are needed, a frequency drift would cause an artificial broadening of the bands. Therefore for accurate results, the drift should be kept at a minimum. For this particular experiment a stability of 50MHz/hr is within the limits of experimental error.

The above stability requirements of the laser system are necessary, but stability must be maintained in the other components of the experiment as well. In high resolution techniques an interferometer is normally used.

Since the operation of an interferometer requires an exact spacing of its mirror (on the order of $\lambda/2$ or less), it is very susceptible to thermal and mechanical oscillations. Therefore, the above instabilities must be controlled such that they produce drifts in frequency that are compatible with the laser system.

Due to low light level, a means of enhancing the detection of the spectrum is necessary. There are two primary methods in signal acquisition that can be used here. First long running times can

increase the quantity of light collected. A photon counting tube and system could be added to further aid the light collection. Secondly, a multi-scan analyzer with the ability to average out random signals could be utilized. The additional requirement needed to measure density fluctuations lies within the interferometer. To measure these fluctuations, the interferometer must act like a very narrow bandpass filter and select a single frequency within the Rayleigh-Brillouin spectrum. In order to accomplish this, the interferometer should be prebiased at a particular frequency by applying a single voltage to the piezoelectric drive.

IV - EXPERIMENTAL EQUIPMENT

The experimental setup is seen schematically in Fig. 5 and pictorially in Fig. 6. During this experiment, two laser systems were used. The first system consisted of a Control Laser Model 554A argon-ion laser pumping a Coherent Model 590 dye laser. The unique property of most dye lasers is that its wavelength is variable. The wavelength selection is accomplished by changing the angular orientation of a birefringent filter. This filter is internally mounted (see Fig. 7) and can be moved by turning a micrometer type adjusting knob. Using all lines of the argon-ion laser, which amounted to about 8 watts, on the dye laser produced approximately 1.4 watts. However, the incorporation of an intracavity etalon system (see Fig. 7) into the dye laser which is necessary to reduce the line width to the specified 10MHz, reduced the power to about 300-500mW. As it turned out, this interferometer only reduced the power available. It did not reduce the line width to the specified bandwidth for any appreciable period of time. The stability was such that it was found useless for the pur-

pose at hand.

The second laser system was just the argon-ion laser itself. The specifications called for approximately 3.5 watts single moded radiation at 514.5 nanometers. This turned out to be an empty claim. To reduce its bandwidth, an intracavity etalon was installed. Since it is characteristic of argon-ion lasers to give off a large amount of heat, the laser utilizes a water jacket for cooling.

Regardless of the source of illumination used, the laser light was directed toward the scattering volume by a Newport Research Corporation Model 670 beam steering mirror. The mirror is able to adjust the angular, horizontal and vertical position of the incident light. The need for this precision mirror was justified by the extreme dependence of the experiment on an accurate alignment. To fulfill this requirement the beam had to be positioned exactly. This was sometimes difficult since it was often necessary to peak the laser to its optimum power level. By doing this, the spatial position shifted slightly. Therefore the mirror was needed to redirect the beam to its rightful course.

To investigate a pure substance a pressure cell was constructed. There was nothing unique about the cell. It was constructed of aluminum with a port on each face. To further reduce the effects of reflection, the cell was black anodized and the windows anti-reflection coated. The latter was not performed until much later in the investigation. The reason being it was not known how much the reflections affected the background photon count.

The light scattered from the material in question was collected by a 5cm diameter, 5cm focal length lens. To produce a point image of the scattering volume, the lens was positioned two focal lengths

from the scattering volume. At this point, an adjustable iris was placed. This was to act as a spatial filter and limit the collected light to that coming from the scattering volume. Another 5cm lens was placed 5cm from the iris, to produce a collimated beam of light.

To frequency filter the scattered light, A Burleigh Model RC-110 interferometer was used. As a means of frequency scanning, a piezoelectric drive was utilized. Since this model incorporated plane mirrors the free spectral range (FSR) could be varied. The FSR could be varied from 1GHz to 15GHz by varying the mirror spacing from 15cm to 0.1cm. Because the parallelity of the mirrors is highly temperature dependent, the interferometer was kept in a thermally insulated, heated box. This box kept the interferometer at a constant temperature, $22 \pm .05^{\circ}\text{C}$.

As in all light scattering techniques a means of low light level detection is necessary. Here a RCA C31034-01 photon counting photomultiplier tube was used.

To reduce the background count and to electromagnetically shield the photomultiplier tube, the tube was housed in a Pacific Photometric thermoelectric cooler. Typically a noise of 300 counts per second at a cathode voltage of 1800 volts was observed.

As a means of signal processing several systems were used. The system primarily utilized was a Princeton Applied Research (PAR) photon counting system. It consisted of a model 1121 amplifier-discriminator and a model 1112 photon counter-processor. This system is capable of monitoring two input channels, by the use of a gated sampler. The two signals can then be either added or subtracted. The result is either displayed digitally or interfaced to a computer system.

During a short time span two other systems were used. These were Princeton Applied Research Model 4202 signal averager and Model 162 boxcar integrator. The first can accumulate data from repetitive scans. Thus the result is the average of all scans received by the unit. This averaging process can be several types; normal, summation and exponential.

The boxcar integrator provided similar results by a different method; after a series of scans are accumulated, the complete data is integrated to produce a single sweep where the random signals are integrated out.

V - GAS SAMPLE PREPARATION AND TECHNIQUE

To minimize the effects of dust and the presence of other gases the test chamber was evacuated and filled several times. A Veeco vacuum pressure transducer recorded a pressure of 20 microns absolute during the evacuation of the chamber. As an added precaution the gas sample was passed through a Matheson gas filter to eliminate dust particles.

The cell was usually pressurized between 50-70 psia. This pressure was measured by a Heise mechanical pressure gauge.

Before and during the experimental test runs the laser's bandwidth was monitored by a Jodon Model 1500 spectrum analyzer.

In monitoring the density fluctuations, a modification in the usual operation of the interferometer was needed. To monitor the fluctuations one frequency must be selected. This can be accomplished by presetting the piezoelectric drive at a particular voltage. At this point the interferometer mirror spacing is fixed and therefore it will only transmit light at one frequency. The value of this particular voltage can be obtained by simultaneously measuring

the spectral response of the laser light source, Fig. 8A, and the voltage applied to the interferometer, Fig. 8B. From this one can select any frequency by picking a particular voltage. The voltage selection depends on the region concerned. In the hydrodynamic region the obvious choice is the voltage at which the maximum intensity occurs. In the kinetic region a voltage should be selected which is free from the effects of the central component. A fair estimate of this can be obtained by calculating the appropriate shift.

VI - FINDINGS

The primary concern of this investigation was to assess the potential of Brillouin scattering as a diagnostic tool. As a first step toward this goal, a spectrum from a sample substance was sought. This would lay the ground work for later work by indicating the troublesome areas.

Although this investigation could not produce a Brillouin spectrum, the shortcomings of this method as a means of measuring instantaneous density fluctuations still surfaced. By analyzing the reasons for failure to detect the scattering process these shortcomings become visible. Therefore a brief discussion of the problems encountered will be given first. Then the shortcomings will be discussed in the conclusion.

As stated before, an earlier study⁴ attempted to measure density fluctuations in liquids. The results obtained from this investigation are given in Figs. 11 and 12. From these results the impact of the impurities present in the liquid could be seen. They produce a level of noise that makes the detection of the spectrum very difficult. Also, due to the inferior quality of the interferometer, this noise

could not be filtered out. It was for these reasons that new equipment was acquired. With this equipment a new study was undertaken. The results of this study are given below.

In the first experimental setup the dye laser system (argon-ion and dye laser), Burleigh interferometer and PAR photon counting system was utilized. These instruments were mounted on two work benches fitted with 1-inch thick aluminum table tops. It took seven-eight months to get the two lasers operating simultaneously. The problem here was the argon-ion power instability; and improper dye laser mirror and jet alignment. To correct these defects, a new argon-ion laser was obtained and the dye laser was shipped back for a proper alignment.

As an initial check-out procedure of the dye laser, a preliminary examination of the laser line width was undertaken. The line width was measured using the Burleigh interferometer. An example of this spectral display is seen in Fig. 9. Here the FSR is 3GHz. Therefore the laser line width is measured to be approximately 250 MHz. This is not indicative of the best value achievable. A bandwidth slightly under 100MHz has been obtained. Even this value is far above the specifications set by the manufacturer. The reason for this will be discussed shortly. Even this "narrow" line width could not be maintained for an appreciable time period. The line width had a tendency to broaden and drift in position. This drift would cause the number of orders to vary. Therefore it would vary the number of Rayleigh lines per sweep. Also the laser line broadening would make the central peak appear wider than it should. Not only did the line width degenerate, but the intensity varied. Ascertaining these variations as a function of time proved to be difficult if not an impossible proposition. The

power meter used for this purpose had too large a response time to indicate the actual deviation. As far as the apparent frequency drift and spectral line broadening are concerned, it is not known to what extent the temperature instability of the interferometer was responsible. Making the assumption that the insulated thermal box of the interferometer provided a better degree of stability, one must conclude that the time stability of the laser was at most ten minutes.

The above instabilities were primarily due to thermal and mechanical induced vibrations. The thermal effects present in the dye laser would allow the etalons to creep and thus destroy their parallelism. These temperature effects were the result of room temperature gradients. The causes of the mechanical vibrations were more difficult to detect. These were discovered to originate from the argon-ion's high voltage power transformer, pulsating cooling water, and the dye laser's dye pump. The most damaging of these was the water supply and dye pump. The reason being the vibrations were transmitted thorough their respective supply lines which are connected directly to the lasers. A flexible tygon hose was connected in series with the dye supply line. This relieved some of the vibration but not all. What was really needed was a means of completely isolating the system from all these effects. This could be accomplished if the system was set on a vibration absorbing lab table. Due to their exorbitantly high cost one could not be obtained at that time. Hence, the experiments had to be run during the brief periods of "stability". These periods were either infrequent or not long enough to produce satisfactory results.

The results that were obtained indicated a high background read-

ing. It was assumed either a misalignment in the optical system or a spatial laser drift caused the unusually high background count. Actually these effects are strongly coupled and both probably contributed simultaneously as well as separately. The laser drift could not be helped. It was a fact that one had to contend with. The high background count was thus the result of reflections and Mie scattering from impurities. Their effects could not be filtered out so readily by the interferometer since they are of the same wavelength and are orders of magnitude large in intensity. Further light baffels and traps were needed and incorporated.

It was at this time a new experimental area was obtained. In this area was a device that appeared that would solve the majority of the problems encountered. This device was a 17,000 pound steel table that measured 12 feet by 4 feet. It had the ability to isolate disturbances transmitted via the ground [since it could be supported by 16 inflated aircraft inner tubes].

The results that followed didn't appear any different than those obtained earlier. These results were still prone to laser instability and high background count. It was discovered the vibrations still prevailed. These vibrations were not damped out by the table because they were transmitted through the supply lines and not the ground. Also the temperature effects were still present. There was no means of eliminating them other than temperature controlling the system or the room.

Since it appeared that the dye laser system could not be used because of its instability, the decision was made to use solely the argon-ion laser with its inter-cavity etalon. Initially the laser was not chosen for this purpose. Therefore no real consideration was

given to the etalon's performance. To obtain some information on its performance, an inquiry was made of the manufacturer. Their reply was not too favorable. They had no specifications as to its exact performance. Also they reluctantly divulged that due to its poor performance (stability and selectivity) they are considering removing it from sales.

Since no good information was available, some measurements were made. The laser line width was measured to be between 125-150 MHz. An example of this is seen in Fig. 10. Here the bandwidth is measured to be 125MHz. This system was a little more stable than the dye laser system. Again it was too difficult to determine the degree of stability and only an estimated time of 10-15 minutes could be assumed. Frequency stability was greatly affected by the large amounts of heat radiating from the laser. Thermal equilibrium could never really be reached due to the erratic flow rate of the cooling water. An attempt was made to eliminate the pulsations by installing a large water reservoir in series with the water supply and the laser head. Before the benefits of this system could be assessed, an accident occurred. Somehow the flow stopped to the head and the discharge tube overheated. Accompanied by this overheating was an increase in gas pressure and, therefore, a loss in power. Since there is no means of reducing this pressure, the laser had to be shipped back for repairs. This was only one of many journeys back to the manufacturer. In all there were at least six. Four of these resulted in the return of new lasers because the old ones couldn't be repaired. These trips usually lasted for three-four weeks. When the laser was in operation it had a tendency to lose power. This problem resulted from a thin film deposited in the

Brewster windows by the outgasing of the plastic, which protected these windows. With the use of a dry nitrogen purge system, the formation of this film was eliminated.

The subsequent experimental tests were still plagued with the high background. Many methods to reduce this background were used. Some of them included light baffels, small aperture iris' and black-ended enclosures. The count couldn't be reduced significantly.

Since the above procedure proved unsuccessful, other means of eliminating this background was sought. Considering the background count as a random process, then a method of averaging would reveal only the signal present. This type of signal processing would however defeat the purpose of this investigation. One has to remember that the purpose of this investigation was to measure the fluctuations of the density in a flow field. To this end, a boxcar integrator and a multi-scan analyzer were acquired. These units were on loan and therefore the time they were available was limited. A combination of this limited time and the infrequency of the laser stability contributed to the failure of this attempt.

VII - CONCLUSION

Upon examination of the findings presented in the previous section, the shortcomings of Brillouin scattering as a diagnostic tool became visible.

First, due to the low light levels either long running times or repetitive scans are necessary. This is obviously unsatisfactory for measuring instantaneous density fluctuations. Next, the usual environment in fluid dynamical experiments is not void of contaminants. These particles would produce an overwhelming response that

would hide the actual signal. Also, the geometrical bodies and configurations usually used would make it impossible to eliminate light due to reflections. In addition to the above reasons, there is the expense and practicality. It would cost a considerable amount to isolate the system vibrationally. This cost does not appear to be of practical use when other methods are available. Finally, there is a very important point that is not readily visible from the results presented. Since the interferometer is unstable in the scanning mode, there is no reason to expect it would be stable in the preset mode. The instability would cause a drift which in turn would allow the intensity to vary. This variation could be interpreted as a fluctuation in density which is erroneous. Therefore with the equipment presently available, the use of Brillouin scattering as a diagnostic tool is in doubt.

In conclusion, it seems that Brillouin scattering should be left to those who wish to measure sound speeds, thermodynamic properties (ratio of specific heats, etc.), and transport properties (shear viscosity, bulk viscosity, and thermal conductivity) of fluids.

VIII - REFERENCES

1. Experimental Diagnostics in Gas Phase Combustion Systems:
Progress in Astronautics and Aeronautics, 53, AIAA, (1977).
A) Bowman, Craig T., "Probe Measurements in Flames".
B) Bilger, R.W., "Probe Measurements in Turbulent Combustion".
C) Gunther, R., "Methods for Measuring Turbulence in Flames".
2. Greenspan, M.: "Propagation of Sound in Rarefied Helium".
J. Acc. Soc. Amer., 22, 5, (1950).
3. Greenspan, M.: "Propagation of Sound in Five Monatomic Gases".
J. Acc. Soc. Amer., 28, 4, (1956).
4. Laiosa, J.: "Preliminary Investigation of Density Fluctuation Measurements Utilizing Brillouin Scattering". M.S. Thesis, Polytechnic Institute of New York (1976). Also appeared as Progress Report, "The Application of Brillouin Scattering to Flow Field Diagnostics, A Preliminary Report", (Feb., 1977).
5. Brillouin, L.: "Diffusion of Light and of X-rays by a Transparent Homogeneous Body". Ann. dePhysique, 17, p. 88, (1922).
6. Komarov, L.I. and Fisher, I.Z.: "Zh. Eksperim i Fear". Fiz. 43, 1927 (1962) (English Translation: Soviet Phys. JETP 16, 1358, (1963)).
7. Van Hove, Phys. Rev. 95, 249 (1954).
8. Yip, S. and Nelken, M.: "Application of a Kinetic Model to Time-dependent Density Correlations in Fluids". Phy. Rev. 135, 5A, p. A1241, (1964).
9. Sugawara, A., Yip, S., Sirovich, L.: Phys. Fluids 11, 925 (1968).
10. Hammond, C.: "Rayleigh-Brillouin Scattering from a Polyatomic Gas". PHd. Thesis Penn. State Univ., (1976).

11. Lao, Q.: "Rayleigh-Brillouin Scattering in Gases and Binary Gaseous Mixtures". PHd. Thesis, State University of N.Y. at Stony Brook, (1975).
12. Hunt, F.V.: AIP Handbook, edited by D.E. Gray, McGraw Hill, N.Y., Chap. 3c, p. 3-33, (1957).
13. Mountain, R.D.: "Spectral Distribution of Scattered Light in a Simple Fluid". Rev. Mod. Phys., 38, 1, (1966).
14. Sugawara, A., Yip, S., Sirovich, L.: Phys. Fluids, 11, pp.19-21, (1968).
15. Sugawara, A., Yip, S., Sirovich, L.: Phys. Fluids, 11, pp.22-23, (1968).
16. Krukis, G.: "Sound Propagation in Binary Gas Mixtures". M.S. Thesis, Polytechnic Institute of Brooklyn, (1970).

IX - BIBLIOGRAPHY

1. Mountain, R.D.: "Interpetation of Brillouin Spectrum". J. Chem. Phys 44, 832 (1966).
2. Mountain, R.D.: "Thermal Relaxation and Brillouin Scattering in Liquids". J. Res. N.B.S., 70A, 3, (1966).
3. Boley, C.D., Desai, R.C. and Tenti, G.: "Kinetic Model and Brillouin Scattering in a Molecular Gas". Can. J. Phys, 50, 2158, (1972).
4. Tenti, G., Boley, C.D., and Desai, R.C.: "On the Kinetic Model Description of Rayleigh-Brillouin Scattering from Molecular Gases". Can. J. Phys, 52, 4, (1974).
5. Tenti, G., Desai, R.C.: "Kinetic Theory of Molecular Gases I: Models of the Linear Walsmann-Snider Collision Operator". Can. J. Phys, 53, 1266, (1975).
6. Tenti, G., Desai, R.C.: "Kinetic Theory of Molecular Gases II: Calculation of Time Dependent Correlation Functions". Can. J. Phys, 53, 1279, (1975).

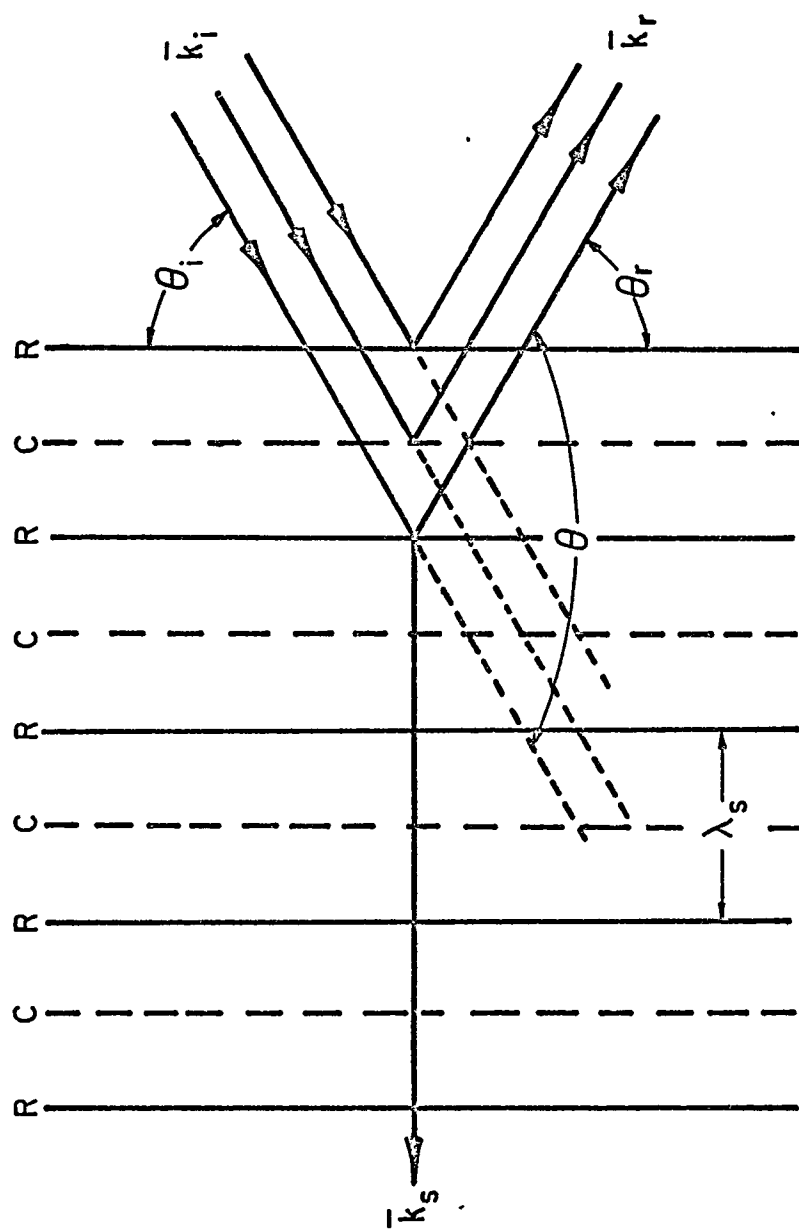


FIG.1 THE STRATIFIED MEDIUM MODEL AND THE "COHERENT REFLECTION" OF LIGHT

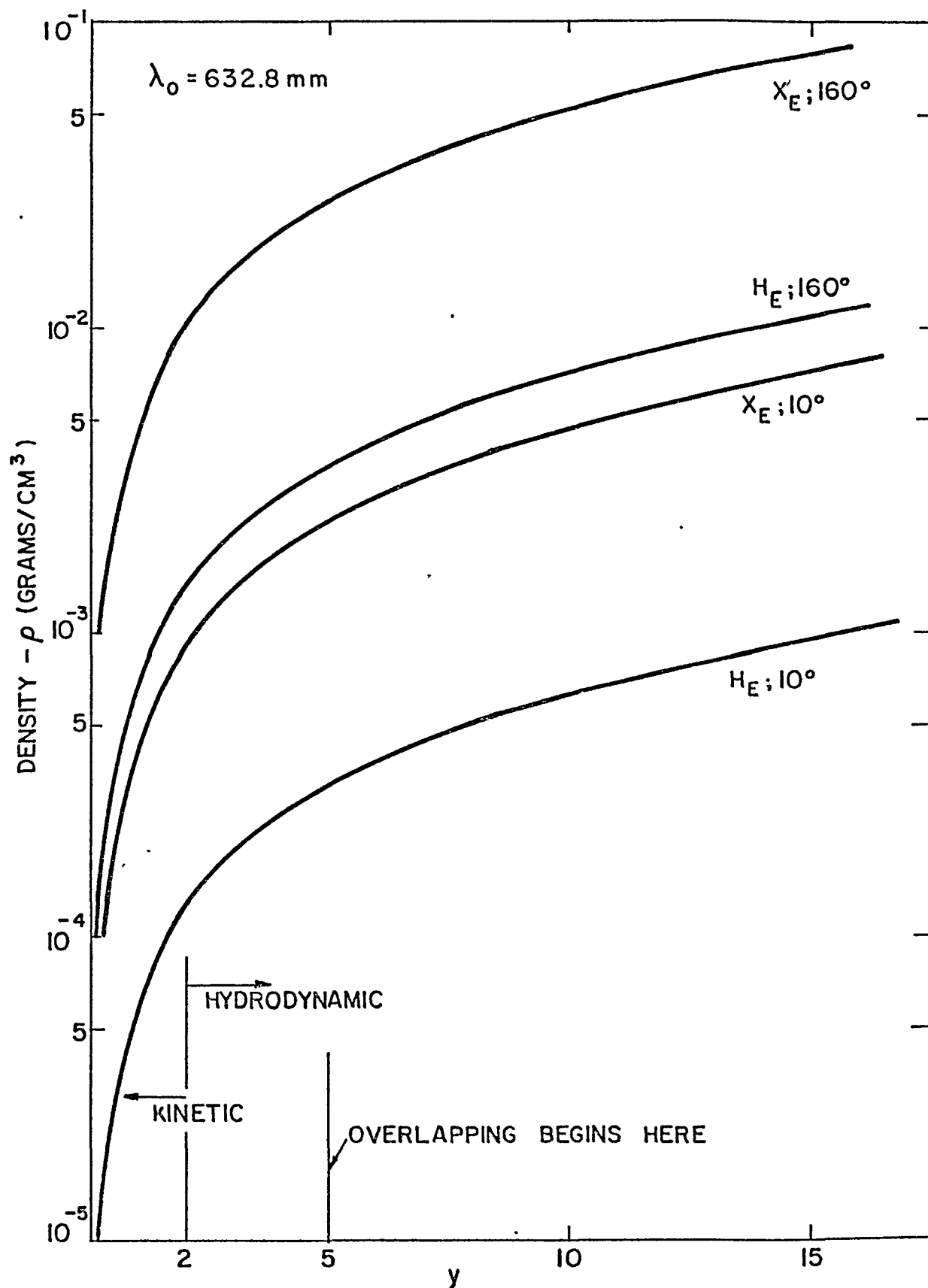
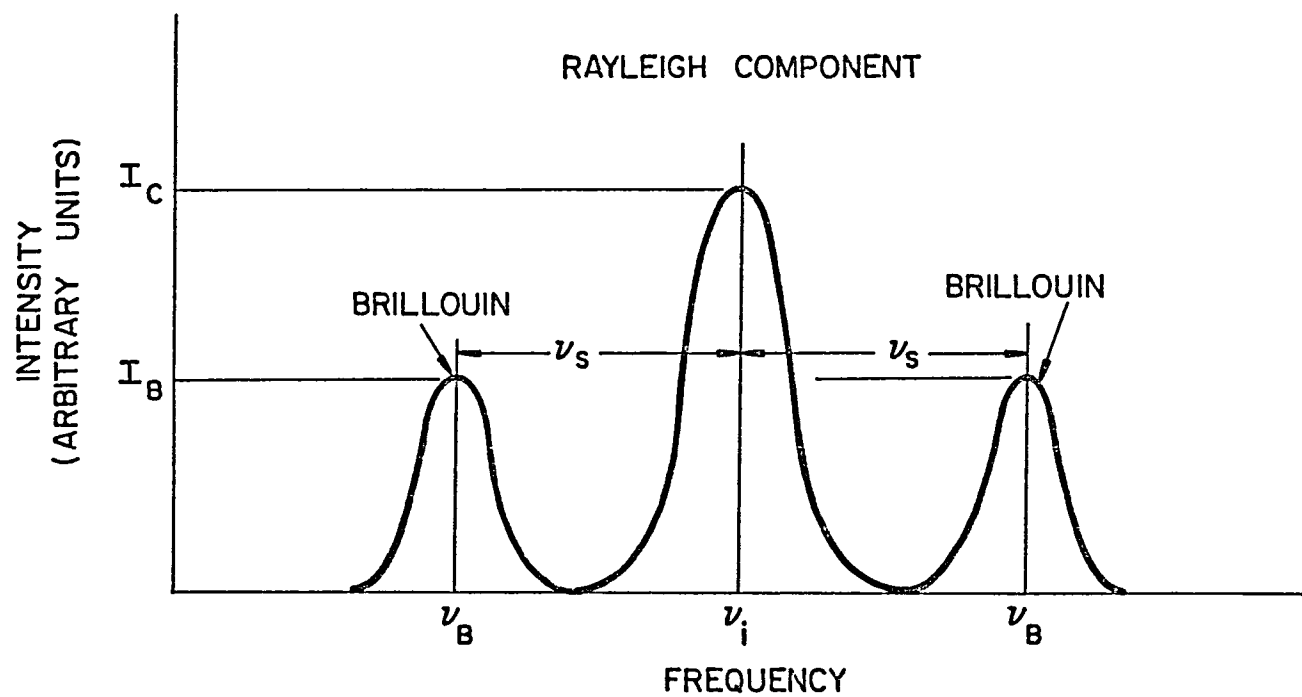


FIG. 2 LIMITS OF THE HYDRODYNAMIC & KINETIC REGIONS FOR HELIUM AND XENON AT VARIOUS SCATTERING ANGLES



**FIG. 3 THEORETICAL HYDRODYNAMIC
BRILLOUIN SPECTRUM**

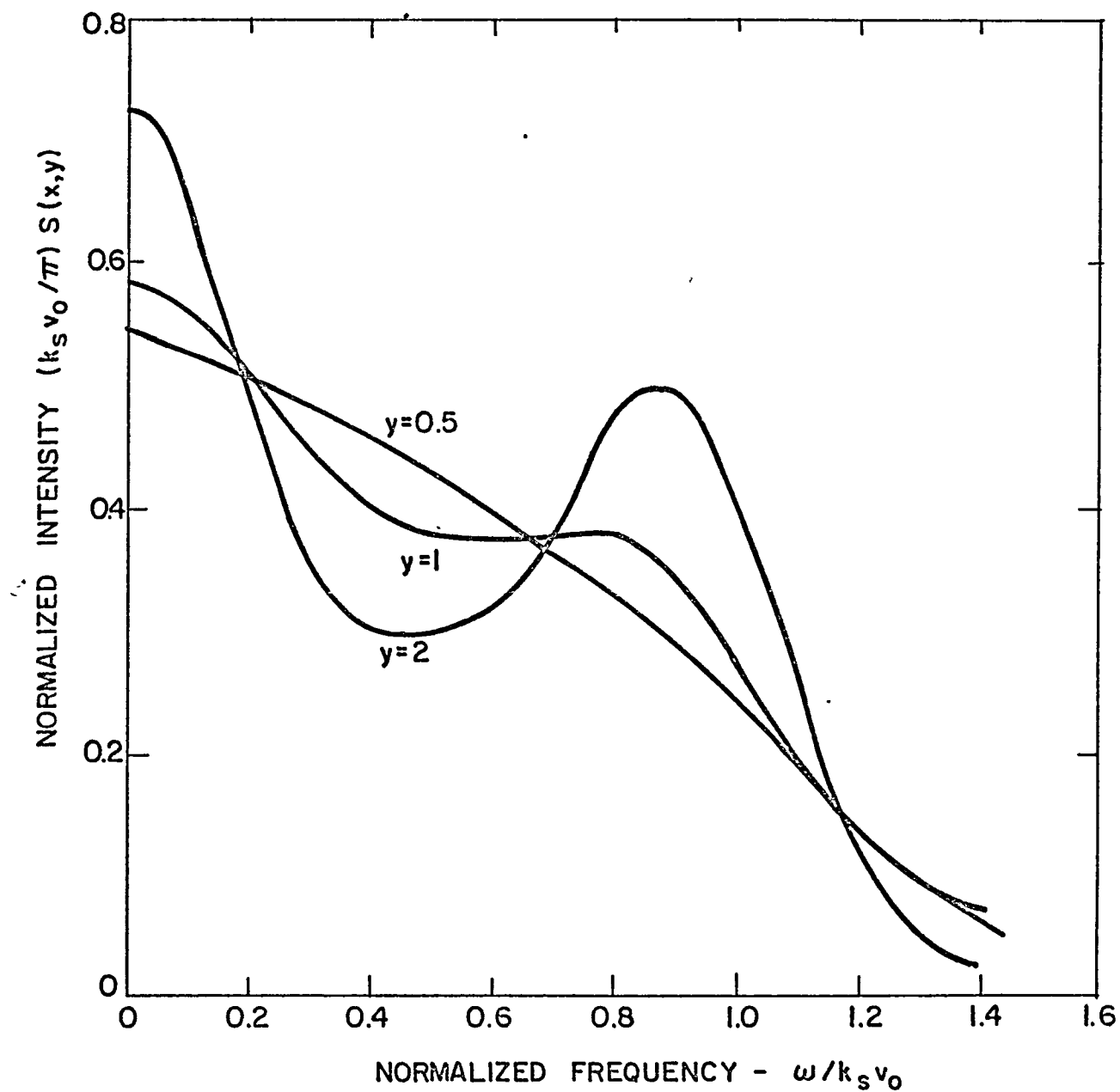


FIG. 4 BRILLOUIN SPECTRUM AS A
FUNCTION OF γ (FROM REF. 4)

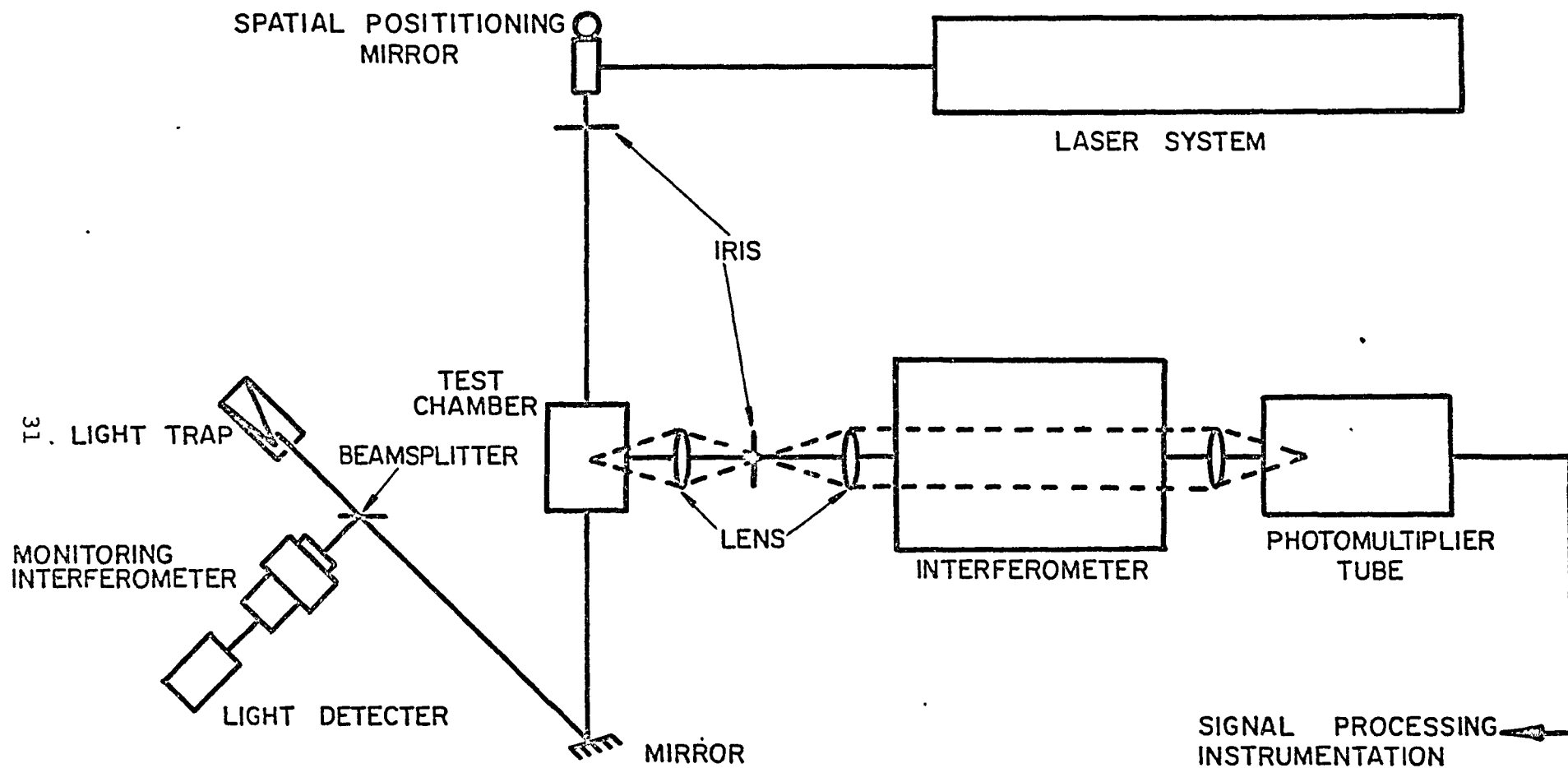


FIG. 5 SCHEMATIC VIEW OF THE EXPERIMENTAL EQUIPMENT

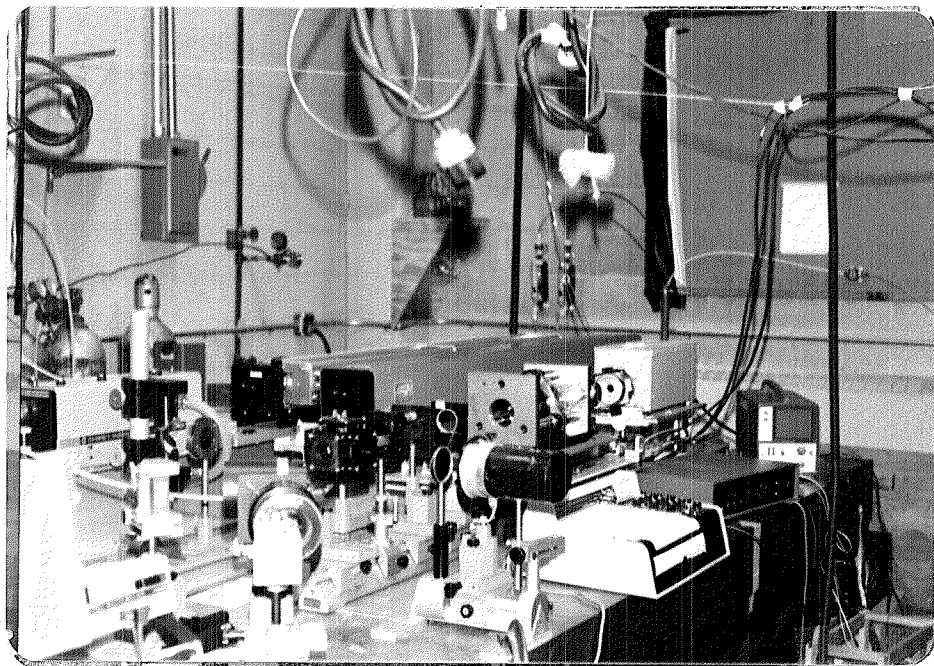
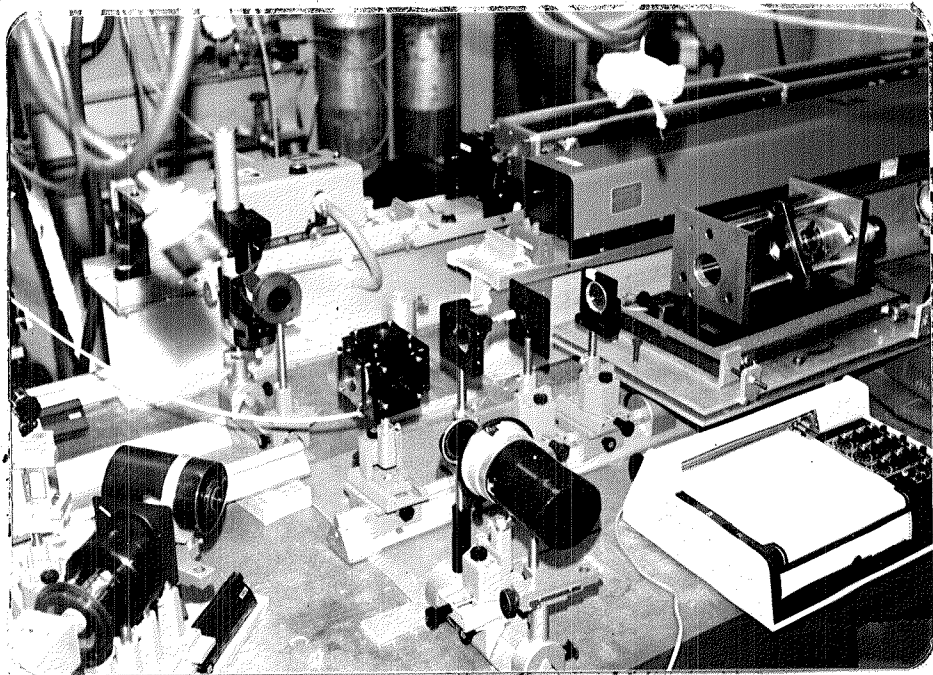


FIG. 6 PICTORIAL VIEW OF THE EXPERIMENTAL EQUIPMENT

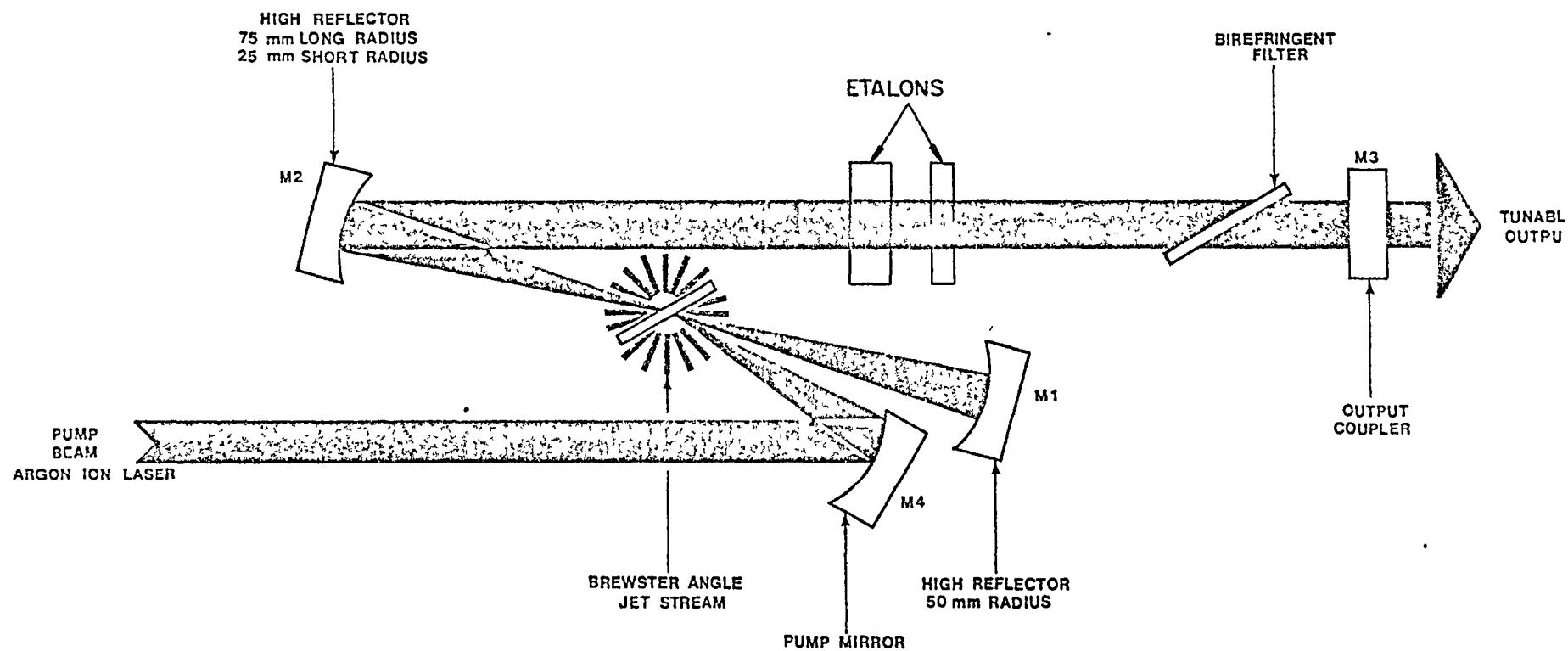
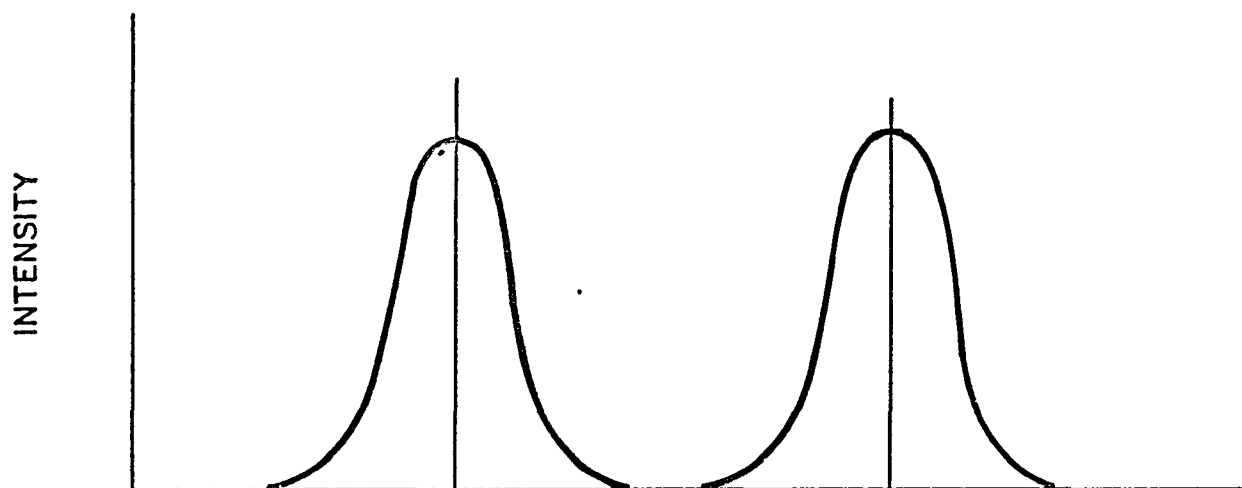
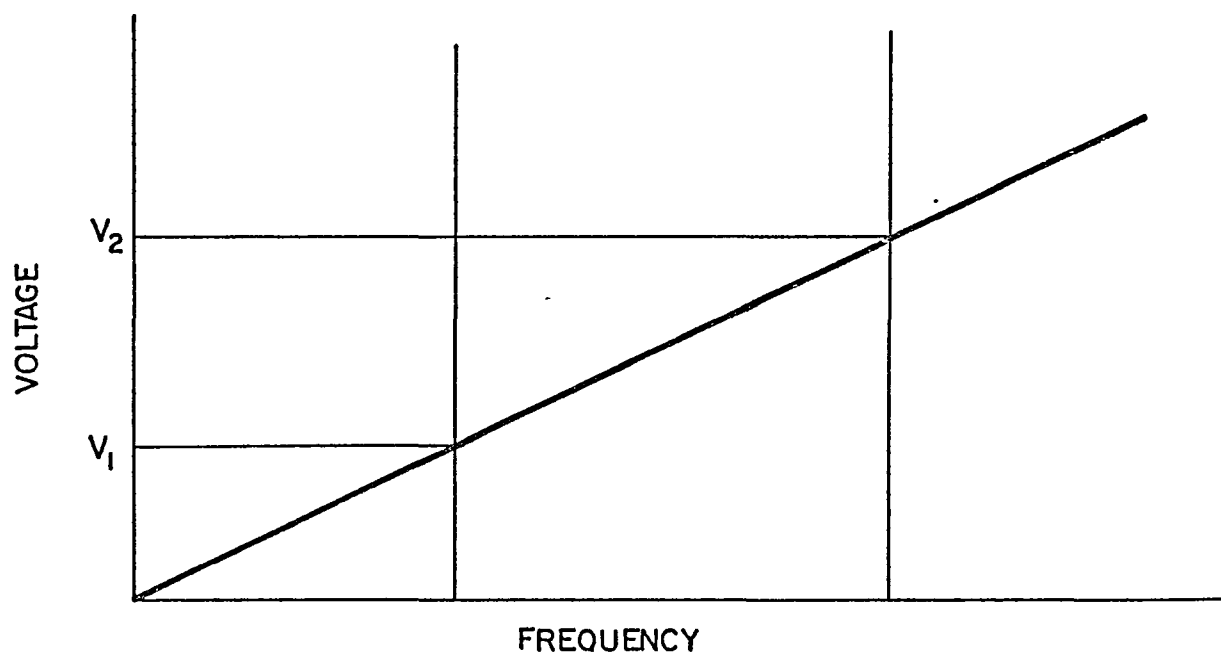


FIG. 7  Model 590 Jet Stream Dye Laser
Optical Schematic



a) SPECTRAL DISPLAY OF THE LIGHT SOURCE BY THE FABRY - PEROT



b) PRESETTING CALIBRATION CURVE

FIG. 8 PRESETTING THE FABRY - PEROT INTERFEROMETER

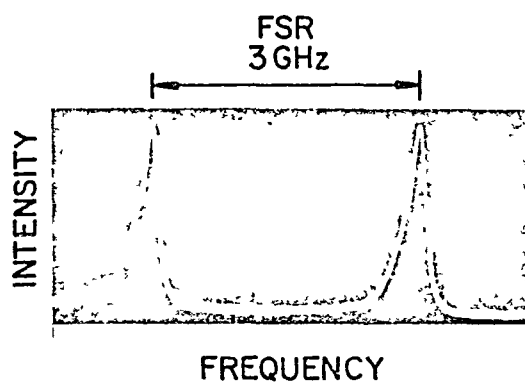


**FIG. 9 SPECTRAL RESPONSE OF DYE LASER; FREE SPECTRAL RANGE IS 3GHz.
LASER BANDWIDTH AT HALF INTENSITY IS 250 MHz.**

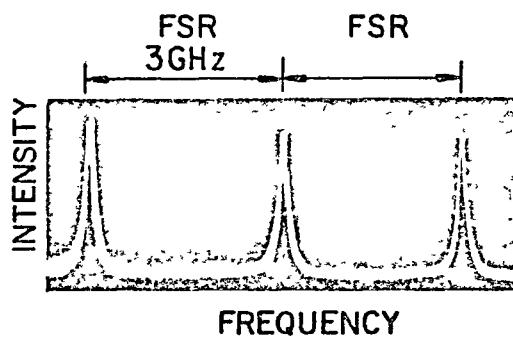


**FIG. 10 SPECTRAL RESPONSE OF
ARGON-ION LASERLINE.
LASER BANDWIDTH AT HALF
INTENSITY IS 125 MHz.**

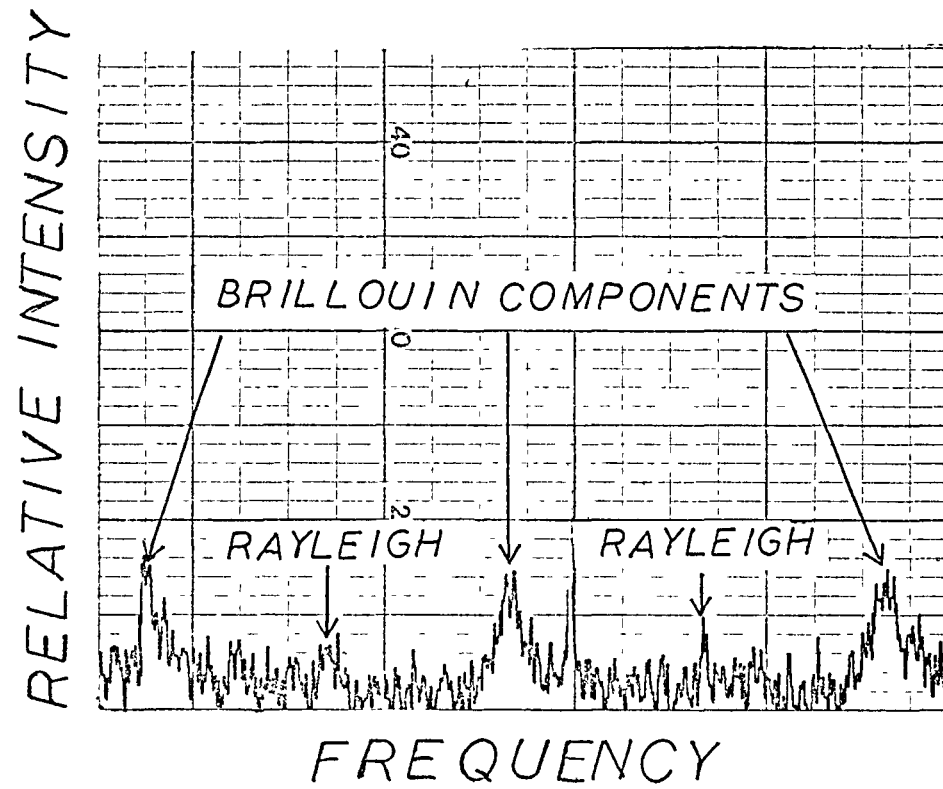


FIG. II. APPARENT SPECTRUM OBTAINED FROM WATER
(TAKEN FROM REF 4)

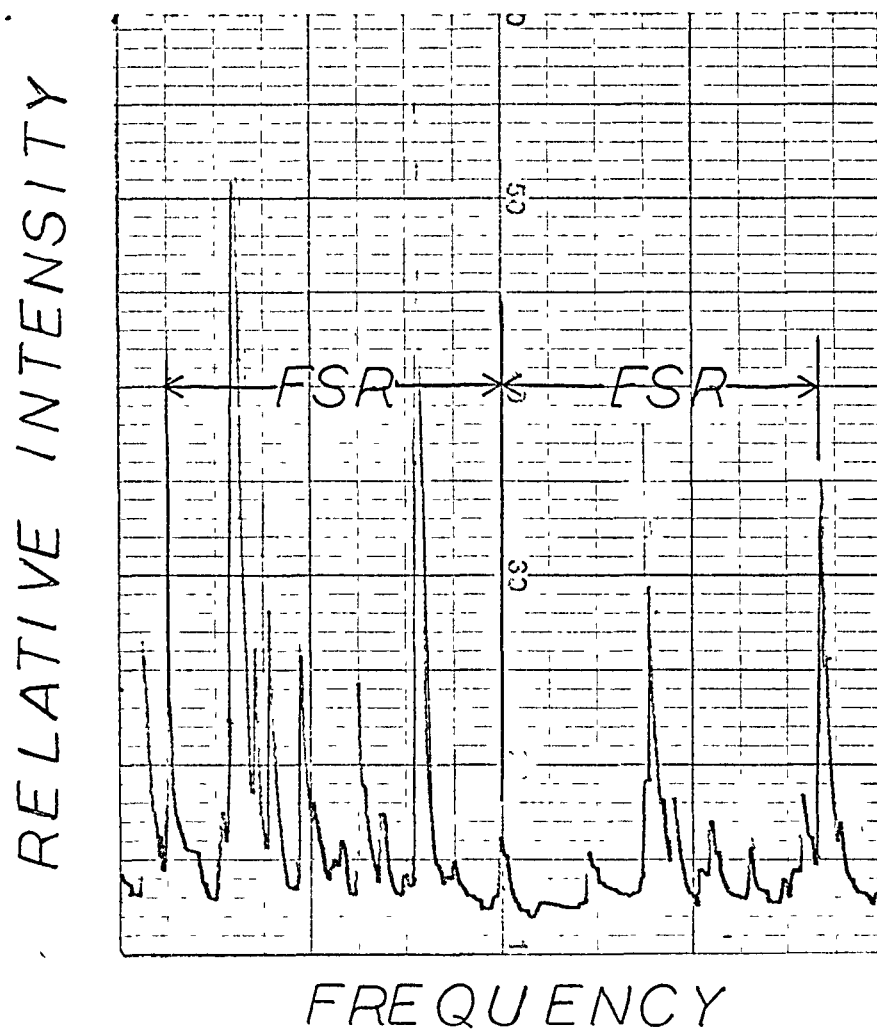


FIG.12 SPECTRAL RESPONSE FROM ABSOLUTE ALCOHOL
(TAKEN FROM REF. 4)

End of Document